

AN EXTENDED STAR CLUSTER AT THE OUTER EDGE OF THE SPIRAL GALAXY M 33¹

Rima Stonkutė², Vladas Vansevičius², Nobuo Arimoto^{3,4},
Takashi Hasegawa⁵, Donatas Narbutis², Naoyuki Tamura⁶,
Pascale Jablonka⁷, Kouji Ohta⁸, and Yoshihiko Yamada³

ABSTRACT

We report a discovery of an extended globular-like star cluster, M 33-EC1, at the outer edge of the spiral galaxy M 33. The distance to the cluster is 890 kpc, and it lies at a 12.5 kpc projected distance from the center of M 33. Old age ($\gtrsim 7$ Gyr) and low metallicity ($[\text{M}/\text{H}] \lesssim -1.4$) are estimated on the basis of isochrone fits. Color-magnitude diagrams of stars, located in the cluster's area, photometric and structural parameters of the cluster are presented. Cluster's luminosity ($M_V = -6.6$) and half-light radius ($r_h = 20.3$ pc) are comparable to those of the extended globular clusters, discovered in more luminous Local Group galaxies, the Milky Way and M 31. Extended globular clusters are suspected to be remnants of accreted dwarf galaxies, and the finding of such a cluster in the late-type dwarf spiral galaxy M 33 would imply a complex merging history in the past.

Subject headings: galaxies: individual (M 33) — galaxies: star clusters

¹Based on data collected at Subaru Telescope, which is operated by the National Astronomical Observatory of Japan

²Institute of Physics, Savanorių 231, Vilnius LT-02300, Lithuania

³National Astronomical Observatory of Japan, Mitaka, Tokyo 181-8588, Japan

⁴Department of Astronomy, Graduate University of Advanced Studies, Mitaka, Tokyo 181-8588, Japan

⁵Gunma Astronomical Observatory, Agatuma, Gunma 377-0702, Japan

⁶Subaru Telescope, National Astronomical Observatory of Japan, 650 North A'ohoku Place, Hilo, HI 96720, USA

⁷Université de Genève, Laboratoire d'Astrophysique de l'Ecole Polytechnique Fédérale de Lausanne (EPFL), Observatoire, CH-1290 Sauverny, Switzerland

⁸Department of Astronomy, Kyoto University, Kyoto 606-8502, Japan

1. Introduction

Resolved stellar diagnostics has been extensively applied for investigation of merging history of galaxies. In this context extended stellar systems have been recently known to be informative. Firstly, some of the extended stellar systems in the Milky Way (MW), e.g., M 54 and ω Cen, are suggested to be remnants of accreted dwarf galaxies, which might be responsible for the thick disk and halo formation. Such systems have produced large-scale stellar streams in the MW, thus they are useful to highlight various substructures of the host galaxies and to reveal their merging history. Secondly, while the key physical processes that discriminate extended star clusters and low surface brightness dwarf spheroidals (dSphs) are poorly understood, their distinction is rather ambiguous.

Searches for extended stellar systems discovered at least a dozen of low surface brightness dSphs in the vicinity of MW (Sakamoto & Hasegawa 2006; Belokurov et al. 2007; Irwin et al. 2007) and M31 (Martin et al. 2006). Recently Huxor et al. (2005) and Mackey et al. (2006) discovered four extended luminous star clusters in the vicinity of M31. Star clusters of this type are also found in the spirals M51 and M81 (Chandar et al. 2004), and in the giant elliptical galaxy NGC 5128 (Gómez et al. 2006). It is important to stress, however, that all extended star clusters found so far belong to massive luminous galaxies. Therefore, any piece of evidence on extended stellar systems in smaller galaxies would play an important role in disclosing the merging history of galaxies on all scales.

M33 is a unique late-type (Scd) dwarf spiral galaxy in the Local Group, resolvable by ground-based observations, and it is claimed (Ferguson et al. 2006) to possess an unperturbed stellar disk without any remarkable sign of thick disk and halo. However, Chandar et al. (2002) revealed an old cluster population, which has a velocity distribution that they attributed to the thick-disk/halo component. Warp of the M33 gaseous disk has already been known from HI observation (Corbelli et al. 1989), and a stellar stream was suggested recently from spectroscopy of individual stars (McConnachie et al. 2006). Any further evidence on the M33 perturbation and accretion events is indispensable to disclose the real formation history of the galaxy. Since stellar systems of accretion origin are often found far from the hosts' central part, wide and deep searches for such objects are crucial.

We report a discovery of an extended star cluster, M33-EC1, in the M33 photometric survey (P.I. N. Arimoto) frames obtained on Subaru Telescope (Fig. 1). The cluster is located at R.A. = $01^h32^m58^s.5$, Decl. = $29^\circ52'03''$ (J2000.0), lying far south from the M33 center at a projected galactocentric distance of $48.4'$. Previous M33 cluster studies did not reveal any clusters of a comparably large size (Chandar et al. 1999, 2001). An extensive catalogue of M33 star clusters recently compiled by Sarajedini & Mancone (2007) does not include this new object.

In section 2 we present details of observations and data reduction. In section 3 the derived cluster parameters and resolved stellar photometry results are given. In section 4 we briefly discuss the impact of our finding in the context of galaxy formation.

2. Observations and Data Reductions

Photometric data of the discovered star cluster, M33-EC1, were obtained during the course of the M33 wide field photometric survey performed on Subaru Telescope, equipped with Prime Focus Camera (Suprime-Cam; Miyazaki et al. 2002). Single shot Suprime-Cam mosaic (5×2 CCD chips; pixel size of $0''.2$) covers a field of $34' \times 27'$, and a magnitude of $V \sim 25^m$ is reached in 60 s. Broad-band images: V -band (exposures 5×90 s; seeing $\sim 1''.0$), R -band (5×90 s; $\sim 0''.6$), and I -band (5×200 s; $\sim 0''.8$) were acquired during photometric nights. For standard reduction procedures we used the software package (Yagi et al. 2002) dedicated to the Suprime-Cam data. We employed the DAOPHOT (Stetson 1987) program set implemented in the IRAF software package (Tody 1993) for crowded-field stellar PSF (point spread function) photometry and integrated aperture photometry of the cluster. The PSF stellar photometry on 5 individual exposures in each passband was performed.

Instrumental magnitudes were transformed to the standard photometric system by referring to the published M33 photometric catalogue (Massey et al. 2006). In total 220 stars spanning the I -band magnitude range from 19^m to 21^m and wide color ranges ($R - I$ from -0.15 to 1.3; $V - I$ from -0.25 to 2.5) were selected as local standards. R.M.S. errors of the transformation equations for $V - I$ and $R - I$ colors, and the I -band are less than $0.^m035$ which, taking into account the number of employed stars, assures accurate calibration. Considering the intrinsic calibration accuracy of the standard stars (Massey et al. 2006), we estimate the accuracy of our photometric data to be of $\sim 0.^m015$ at $I = 22^m$. We used a bilinear $R - I$ color transformation equation due to a significant difference between the transmission curve of the Suprime-Cam R -band interference filter and that of the standard Cousins R -band filter.

The star cluster M33-EC1 is located far beyond the M33 galaxy's disk, therefore, it is reasonable to assume that its colors are contaminated only by the MW's foreground extinction. Photometric data were de-reddened using the $E(B - V) = 0.06$ value, derived at the cluster's position from the extinction maps (Schlegel et al. 1998), as follows $A_V = 3.1 \cdot E(B - V)$, $A_I = 0.11$, $E(R - I) = 0.045$.

3. Results

3.1. Color-magnitude diagram

The color-magnitude diagram (CMD) of a region of $20''$ radius, centered on the star cluster M 33-EC1, is dominated by red giant branch (RGB) stars, see Fig. 2. Reduction and photometry procedures enable us to recognize and remove obvious bright non-stellar objects (star/galaxy separation was performed by eye referring to PSF fitting parameters – sharpness and χ^2), however, faint unresolved background galaxies can still be present in this diagram.

In order to resolve well-known age-metallicity degeneracy of the RGB position in CMD, inherent to old populations, it is helpful to introduce faint RGB and horizontal branch stars into the isochrone fitting procedure, see e.g., Martin et al. (2006). The global shape of our CMD resembles the CMD plotted in Fig. 7 from Martin et al. (2006), implying the presence of a very old population with a prominent horizontal branch. However, the limiting magnitude of our observations is too shallow for reliable morphology study of the lower part of the CMD. Therefore, to estimate the intrinsic RGB width over the entire magnitude range, and to derive radial and magnitude dependence of data completeness, we performed an artificial star test (AST) on R - & I -band images. The AST results quantify in detail the photometry errors, confusion limits and data completeness, making the isochrone fitting procedure more robust and better constrained.

Six reference points on the observed RGB ($I, R - I = 20.90, 0.72; 21.90, 0.65; 22.90, 0.57; 23.40, 0.53; 23.90, 0.49; 24.40, 0.46$) were selected to represent the entire magnitude range of the cluster's stellar population. DAOPHOT's *addstar* procedure was employed to add artificial stars to the images. To avoid self-crowding we generated individual AST images at every reference point. Each AST image contains 400 artificial stars of the same magnitude distributed on a regular grid (step $3''$) over the region of $60'' \times 60''$ centered on the cluster. However, only 140 artificial stars fall within the actual cluster radius of $20''$. In order to increase the number of artificial stars and derive radial data completeness distributions more reliably, we generated 21 individual images for each passband and every reference point by shifting the grid around the initial position to 8 and 12 symmetrically distributed locations around the initial position at the radial distances of $\sim 0''.6$ and $\sim 1''.2$, respectively. Therefore, within the radius of $20''$ we used 2940 artificial stars in total at each reference point on the RGB. The photometry procedure of the AST images was exactly the same as the one employed for the real star photometry.

To understand the morphology of star distribution in the lower part of CMD we constructed artificial star CMD. Radial distribution of the artificial stars at every reference AST

point on the RGB was chosen to represent the observed radial density distribution of the cluster stars. However, to increase robustness of the artificial star CMD, we used a number of artificial stars 5 times greater than the number of real stars. The observed cluster stars over-plotted on the artificial star CMD are shown in Fig. 2, panel b).

“Christmas tree-like” artificial star CMD (Fig. 2, panel b) implies that CMD of the star cluster M 33-EC1 is composed solely of RGB stars, experiencing very low contamination by foreground stars and background galaxies. Note, however, the enhanced (in respect to the artificial stars) density of the faint blue ($R - I < 0.25$) objects, which could be attributed to horizontal branch stars of the cluster or faint blue galaxies. Therefore, the straightforward isochrone fit to the observed stars can be applied down to $I = 23^m$, using only the RGB part of the isochrones.

We constructed the radial data completeness plot (Fig. 3) by counting the recovered artificial stars in $2''$ wide annulus zones centered on the cluster. Stars down to $I = 23^m$ are well recovered even at the very center of the cluster. At this magnitude level we are able to find and measure more than 70% of the stars at the cluster’s center and more than 95% at larger radii (Fig. 3).

The $\sim 100\%$ data completeness of the brightest RGB stars is of high importance for the cluster’s distance determination by fitting the tip of RGB (TRGB). This method is based on the assumption (valid for $[\text{Fe}/\text{H}] \leq -0.7$ and ages of $\gtrsim 2$ Gyr) that the absolute I -band magnitude of TRGB ($M_I = 4.05 \pm 0.10$) is independent of metallicity and age (Lee et al. 1993; Bellazzini et al. 2001). The AST data completeness results imply that the TRGB method can be applied throughout the radial extent of the star cluster.

A magnitude of the brightest RGB star (it is located within the cluster’s core, however, in an uncrowded area, and thus measured accurately) is of $I = 20.81 \pm 0.01$. Taking into account the MW foreground extinction ($A_I = 0.11$), this converts to a distance modulus of $(m - M)_0 = 24.75 \pm 0.10$ and places the star cluster M 33-EC1 at a distance of 890 ± 40 kpc. The distance modulus error is dominated by the systematic error of the TRGB calibration (± 0.10) and by an additional increase of the distance modulus, arising due to a probability, that the brightest observed star is below the very tip of theoretical RGB, because of a small total number of RGB stars in the cluster.

It is noteworthy to stress, that we determine the RGB tip of the M 33 galaxy’s outer disk at $I = 20.68 \pm 0.02$, which converts, by applying the MW foreground extinction, $A_I = 0.08$, and assuming validity of the TRGB method for the case of M 33 outer disk’s metallicity, to ~ 850 kpc. The derived distance of M 33 is in agreement with recent M 33 galaxy distance determinations, based on the TRGB method, by Galleti et al. (2004) and Tiede et al.

(2004) – 855 kpc and 867 kpc, respectively. However, the detached eclipsing binary method gives a significantly longer distance of 964 kpc (Bonanos et al. 2006), while a cepheid based distance is shorter – 802 kpc (Lee et al. 2002). Therefore, further in this paper we will use the distance modulus of 24.75, which places M 33-EC1 at a projected distance of 12.5 kpc from the M 33 center.

To estimate the cluster’s age and metallicity we compared the shape and slope of the observed RGB with the isochrones of Girardi et al. (2002) and VandenBerg et al. (2006). In the case of Girardi et al. (2002) isochrones, we achieved the best fit for the interpolated isochrone of the age of 13 Gyr and metallicity of $[M/H] = -1.2$ (Fig. 2, panel a; isochrone of the age of 14 Gyr and metallicity of $[M/H] = -1.3$ is over-plotted). However, the isochrone of lower metallicity, $[M/H] = -1.4$, and age of ~ 18 Gyr, as well as the isochrone of higher metallicity, $[M/H] = -1.0$, and age of ~ 2.5 Gyr, can also be fitted reasonably well. Therefore, additional information is needed in order to break the age (2.5–18 Gyr) and metallicity ($[M/H] = -1.4$ – -1.0) degeneracy.

We obtained more constrained fits by employing VandenBerg et al. (2006) isochrones (2–18 Gyr), which are available on the finer metallicity grid for three alpha element abundance ratios ($[\alpha/Fe] = 0.0, 0.3, 0.6$). We achieved good, although degenerate, fits for the ages of >7 Gyr and metallicity of $[M/H] < -1.4$ independent on alpha element abundance, see Fig. 4. The isochrones spanning a narrow age and metallicity range are over-plotted on CMDs for the illustrative purpose. Assuming the reasonably old cluster’s age of 13 Gyr, we derived metallicity of $[M/H] = -1.6$. Note, that for the same age (13 Gyr) metallicity derived from the Girardi et al. (2002) isochrones is higher by 0.4 dex. The derived metallicity $[M/H] \lesssim -1.4$ is in good agreement with the recent spectroscopic metallicity determination of the M 33 halo stars in a nearby field to the M 33-EC1 location (McConnachie et al. 2006).

3.2. Integrated photometry and structural parameters

The M 33-EC1 age of >7 Gyr, estimated from the isochrone fitting, implies that it should possess a globular cluster-like surface number density profile, which is traditionally fitted by the King model (King 1962):

$$\rho(r) = \rho_0 \cdot [(1 + (r/r_c)^2)^{-1/2} - (1 + (r_t/r_c)^2)^{-1/2}]^2,$$

where ρ_0 – central surface number density, r_c – core radius, and r_t – tidal radius are profile fitting parameters. However, due to a small number of bright stars and an incompleteness of the stellar photometry catalogue at fainter magnitudes (see Fig. 3), we decided to fit the

King model to the surface brightness, rather than to the surface number density profile. This assumption is reasonable for the surface brightness profiles, constructed from aperture photometry, which even at large radial distances sample the cluster's stellar population satisfactorily well.

On the other hand, large M 33-EC1 extent and relatively low luminosity (mass), as well as long (~ 12.5 kpc) projected distance from the host galaxy's center, can lead to an assumption, that the cluster is dynamically young and possesses a surface brightness profile, which could be reproduced by the empirical EFF (Elson et al. 1987) profile derived for young (< 300 Myr) Large Magellanic Cloud clusters. We employed the EFF model in differential form representing surface brightness profile

$$\mu(r) = \mu_0 \cdot (1 + (r/r_e)^2)^{-n},$$

and in integral form representing integrated luminosity profile

$$\Sigma(r) = \Sigma_0 \cdot r_e^2 / (n - 1) \cdot [1 - (1 + (r/r_e)^2)^{1-n}],$$

where μ_0 – central surface brightness, Σ_0 – central luminosity, r_e – scale-length, and n – power-law index.

Determination of an accurate center of the well resolved cluster is a sensitive procedure in constructing the surface brightness profile. In the central part of M 33-EC1 luminous stars are distributed slightly asymmetrically (see Fig. 1), therefore, the location of the center was derived by fitting the luminosity weighted and spatially smoothed surface brightness profile in the area of $20'' \times 20''$. M 33-EC1 exhibits perfectly round isophotes at large radii, suggesting that the mass distribution is spherical in general – hence we used circular apertures for the construction of surface brightness and integrated luminosity profiles, by integrating in $0''.4$ wide annuli up to the radius of $20''$.

The sky background was determined in a circular annulus centered on the cluster and spanning the radial range from $20''$ to $30''$ (see Fig. 1). The correct sky background subtraction is critical for determining a shape of surface brightness profile in the cluster's outer region (for detailed discussion see Hill & Zaritsky 2006), therefore, systematic sky background subtraction errors were evaluated by constructing the profiles with over-subtracted and under-subtracted sky background. The sky background variation by R.M.S. of the sky background value, led to insignificant structural parameter changes.

Resultant M 33-EC1 radial surface brightness profiles are smooth up to $\sim 16''$ radius, where a bright RGB star is located. Therefore, we performed the King and EFF model

profile fitting up to the radius of 14''. The best model fits to the V -band sky background-subtracted integrated luminosity (top panel) and surface brightness (bottom panel) radial profiles are presented in Fig. 5.

Directly fitted and derived (r_h and full-width at half maximum, FWHM) M 33-EC1 structural parameters, as well as corresponding standard deviations, are listed in Table 1. Derived parameters were computed basing on transformation equations (6, 7, 9, 10) presented by Larsen (2006) for the EFF profile

$$\text{FWHM} = 2 \cdot r_e \cdot \sqrt{2^{1/n} - 1},$$

$$r_h = r_e \cdot \sqrt{0.5^{1/(1-n)} - 1},$$

and the King profile

$$\text{FWHM} = 2 \cdot r_c \cdot \sqrt{((1 - \sqrt{0.5})/\sqrt{1 + (r_t/r_c)^2} + \sqrt{0.5})^{-2} - 1},$$

$$r_h = 0.547 \cdot r_c \cdot (r_t/r_c)^{0.486}.$$

For further discussion we choose the conservative lower limit of the cluster's half-light radius of $r_H = 4''7$, that, at the estimated distance of 890 kpc, converts to ~ 20.3 pc, revealing the extended M 33-EC1 nature. It is also important to note, that the differences between V -, R -, I -band profile fit parameters are smaller than their standard deviations. Therefore, in Table 1 we give averaged parameters for the three passbands. It is worth noting, that a change of the fitting radius from 12'' to 19'' does not influence the derived cluster parameters significantly. Integrated magnitudes and colors derived at the cluster's center and radii of $(1 - 4) \cdot r_H$ are listed in Table 2. We find no significant color gradient over the entire radial cluster's extent. $V - I$ color of M 33-EC1, taking into account that only foreground extinction is present at this galactocentric distance, is in the color range of the intermediate and old age ($\gtrsim 5$ Gyr) M 33 clusters (Sarajedini & Mancone 2007).

4. Discussion

We report a discovery of an extended globular-like star cluster (eGC) at the outer edge of the M 33 galaxy, M 33-EC1. All the previously known clusters in M 33 are compact ones with core radii of $r_c \lesssim 2$ pc (Chandar et al. 1999, 2001). Therefore, M 33-EC1 with $r_c \sim 25$ pc is of a very rare type, and the only such object found in the Subaru Suprime-Cam wide-field survey frames ($\sim 1^\circ.1 \times 1^\circ.7$) of the M 33 galaxy.

The $r_h - M_V$ diagram was proven to be a very informative and suggestive tool for a star cluster study (van den Bergh & Mackey 2004). In Fig. 6 we plot this diagram, taking representative objects from various studies published recently, and mark M 33-EC1. The MW galaxy has ten exceptionally large ($r_h \gtrsim 15$ pc) globular clusters (Harris 1996). However, only two of them (NGC 5053 and NGC 2419) are of comparable luminosity or brighter ($M_V < -6.5$) than M 33-EC1. Recently, four clusters of such extreme-type have also been found in the vicinity of M 31 (Huxor et al. 2005; Mackey et al. 2006). Huxor et al. (2005) pointed out, that eGCs in the MW are fainter than those in the M 31 galaxy, due to differing formation and evolution scenarios of the host galaxies.

By means of luminosity, structural parameters, and metal-poor nature, M 33-EC1 is very similar to NGC 5053 (MW eGC) and to four M 31 eGCs. Therefore, regardless of the difference in morphological type, size, and luminosity, in the vicinity of three different galaxies eGCs of the same type reside. Similar eGCs discovered in the spirals M 51 and M 81 (Chandar et al. 2004), and in the giant elliptical galaxy NGC 5128 (Gómez et al. 2006) expand further the variety of eGC's host galaxies (Fig. 6). To our knowledge, M 33 is the smallest spiral galaxy hosting eGC.

We note that recent studies (Sakamoto & Hasegawa 2006; Belokurov et al. 2007; Irwin et al. 2007) do not warrant a simple classification of stellar systems by using their structural parameters, therefore, structural parameters of M 33-EC1 may also be shared with low surface brightness dwarf galaxies. In this context, the extended nature and very low concentration ($r_t/r_c \sim 2.5$; Table 1) of M 33-EC1 suggests that this stellar system could be a low surface brightness dwarf galaxy. The central surface brightness of $\mu_{0,V} \sim 23$ mag·arcsec $^{-2}$ is both consistent with lower end of surface brightness of the MW globular clusters (Harris 1996) and with local dwarf galaxies (Mateo 1998). At present, we have no clear diagnostics to discriminate between these possibilities. The best way to constrain the origin of M 33-EC1 would be to conduct a study of cluster dynamics. The velocity dispersion data, in particular, would make it possible to determine whether this cluster contains dark matter or not (Bender et al. 1992), since low surface brightness dSphs are found to exhibit very large mass-to-light ratio, see e.g. Kleyna et al. (2005), Martin et al. (2007).

The extended nature of M 33-EC1 becomes very important when it is considered in light of merging history of M 33. Basing on the assumption that M 33 has no (prominent) thick disk and/or halo (Ferguson et al. 2006), it has long been postulated that very few, if any, massive accretion events have taken place. It is still controversial issue, however, whether M 33 is a pure stellar disk system or it has a thick disk and/or a halo component. It is interesting to note, however, that accumulating evidences suggest a complex merging history of M 33. Chandar et al. (2002) reported that there is a wide spread in the age of star

clusters and some old clusters have velocities consistent with the halo component dynamics. McConnachie et al. (2006) suggested a halo component and a possible stream by means of spectroscopic study of individual RGB stars. The discovered M 33-EC1 cluster may also give support for the merging history scenario – it could be a stripped dwarf galaxy that has accreted and merged onto M 33 – a scenario suggested for eGCs in M 31 (Huxor et al. 2005). We note that the proximity of M 33-EC1 relative to the stream (McConnachie et al. 2006) could suggest a physical connection, however, the preliminary metallicity estimates for both parties differ significantly. We here just mention that the metallicity of globular clusters in Sagittarius dwarf spheroidal do not necessarily agree with that of parent galaxy (Bellazzini et al. 2003).

Vansevičius et al. (2004) discovered an extended halo in the dwarf irregular galaxy Leo A and suggested that even such a small dwarf galaxy was formed in a much more complex way than believed before, implying hierarchical galaxy formation on all scales. Recent findings indicate that small late-type disk galaxies, such as M 33, could have experienced merging events. Therefore, the eGC presented in this paper, M 33-EC1, together with various objects, which are suggested to associate with the M 33 halo, are all important targets for detailed study in order to understand the merging history of not only M 33, but of galaxies on all scales.

We are indebted to Chisato Ikuta for her invaluable help with observations on Subaru telescope. We are thankful to the anonymous Referee for constructive suggestions and proposed corrections. This work was financially supported in part by a Grant of the Lithuanian State Science and Studies Foundation, and by a Grant-in-Aid for Scientific Research by the Japanese Ministry of Education, Culture, Sports, Science and Technology (No. 19540245).

REFERENCES

Bellazzini, M., Ferraro, F. R., & Pancino, E. 2001, *ApJ*, 556, 635
Bellazzini, M., Ferraro, F. R., & Ibata, R. 2003, *AJ*, 125, 188
Belokurov, V., et al. 2007, *ApJ*, 654, 897
Bender, R., Burstein, D., & Faber, S. M. 1992, *ApJ*, 399, 462
Bonanos, A. Z., et al. 2006, *ApJ*, 652, 313
Brodie, J. P., & Larsen, S. S. 2002, *AJ*, 124, 1410

Chandar, R., Bianchi, L., & Ford, H. C. 1999, *ApJ*, 517, 668

Chandar, R., Bianchi, L., & Ford, H. C. 2001, *A&A*, 366, 498

Chandar, R., Bianchi, L., Ford, H. C., & Sarajedini, A. 2002, *ApJ*, 564, 712

Chandar, R., Whitmore, B., & Lee, M. G. 2004, *ApJ*, 611, 220

Corbelli, E., Schneider, S. E., & Salpeter, E. E. 1989, *AJ*, 97, 390

Elson, R. A. W., Fall, S. M., & Freeman, K. C. 1987, *ApJ*, 323, 54

Ferguson, A., Irwin, M., Chapman, S., Ibata, R., Lewis, G., & Tanvir, N. 2006, preprint (astro-ph/0601121)

Galleti, S., Bellazzini, M., & Ferraro, F. R. 2004, *A&A*, 423, 925

Girardi, L., Bertelli, G., Bressan, A., Chiosi, C., Groenewegen, M. A. T., Marigo, P., Salasnich, B., & Weiss, A. 2002, *A&A*, 391, 195

Gómez, M., Geisler, D., Harris, W. E., Richtler, T., Harris G. L. H., & Woodley, K. A. 2006, *A&A*, 447, 877

Harris, W. E. 1996, *AJ*, 112, 1487

Hill, A., & Zaritsky, D. 2006, *AJ*, 131, 414

Huxor, A. P., Tanvir, N. R., Irwin, M. J., Ibata, R. A., Collett, J. L., Ferguson, A. M. N., Bridges, T., & Lewis, G. F. 2005, *MNRAS*, 360, 1007

Irwin, M. J., et al. 2007, *ApJ*, 656, L13

King, I. 1962, *AJ*, 67, 471

Kleyna, F. F., Wilkinson, M. I., Evans, S. N. W., Gilmore, G. 2005, *ApJ*, 630, L141

Larsen, S. S. 2006, An ISHAPE user's guide (ver. Oct. 23, 2006; available at <http://www.astro.uu.nl/~larsen/baolab/>), p. 14

Lee, M. G., Freedman, W. L., & Madore, B. F. 1993, *ApJ*, 417, 553

Lee, M. G., Kim, M., Sarajedini, A., Geisler, D., & Gieren, W. 2002, *ApJ*, 565, 959

Mackey, A. D., et al. 2006, *ApJ*, 653, L105

Martin, N. F., Ibata, R. A., Irwin, M. J., Chapman, S., Lewis, G. F., Ferguson, A. M. N., Tanvir, N., & McConnachie, A. W. 2006, MNRAS, 371, 1983

Martin, N. F., Ibata, R. A., Chapman, S. C., Irwin, M., Lewis, G. F. 2007, preprint (astro-ph/0705.4622)

Massey, P., Olsen, K. A. G., Hodge, P. W., Strong, S. B., Jacoby, G. H., Schlingman, W., & Smith, R. C. 2006, AJ, 131, 2478

Mateo, M. 1998, ARA&A, 36, 435

McConnachie, A. W., Chapman, S. C., Ibata, R. A., Ferguson, A. M. N., Irwin, M. J., Lewis, G. F., Tanvir, N. R., & Martin, N. F. 2006, ApJ, 647, L25

Miyazaki, S., et al. 2002, PASJ, 54, 833

Sakamoto, T., & Hasegawa, T., 2006, ApJ, 653, L29

Sarajedini, A., & Mancone, C. L. 2007, AJ, 133, 447

Schlegel, D., Finkbeiner, D., & Davis, M. 1998, ApJ, 500, 525

Stetson, P. B. 1987, PASP, 99, 191

Tiede, G. P., Sarajedini, A., & Barker, M. K. 2004, AJ, 128, 224

Tody, D. 1993, in ASP Conf. Ser. 52, Astronomical Data Analysis Software and Systems II, ed. R. J. Hanisch, R. J. V. Brissenden, & J. Barnes (San Francisco: ASP), 173

VandenBerg, D. A., Bergbusch, P. A., & Dowler, P. D. 2006, Ap&SS, 162, 375

Vansevičius, V. et al. 2004, ApJ, 611, L93

van den Bergh, S., & Mackey, A. D. 2004, MNRAS, 354, 713

Yagi, M., et al., 2002, AJ, 123, 66

Table 1: Structural parameters of the star cluster M 33-EC1.

Models	r_e	n	FWHM	r_h
EFF (integral)	8.5 ± 0.8	3.6 ± 0.6	7.9 ± 0.1	4.7 ± 0.2
EFF (differential)	10.2 ± 1.3	4.6 ± 1.0	8.3 ± 0.2	4.7 ± 0.1
	r_c	r_t	FWHM	r_h
King (differential)	5.8 ± 0.3	14.6 ± 0.8	8.2 ± 0.2	4.9 ± 0.1

Note. All parameters are given in arc-seconds.

Table 2: Photometric parameters of the star cluster M 33-EC1.

r [r_{H}]	V	$V - R$	$R - I$	M_V	Σ_V [$\text{L}_{V,\odot} \cdot \text{pc}^{-2}$]	μ_V [mag·arcsec $^{-2}$]
0	—	0.47	0.44	—	22.6	23.03
1	19.11	0.47	0.48	-5.83	14.4	23.52
2	18.50	0.47	0.47	-6.44	6.3	24.42
3	18.39	0.48	0.46	-6.55	3.1	25.19
4	18.33	0.49	0.46	-6.61	1.8	25.75

Note. Distance from the cluster's center, r , is given in cluster's half-light radius, $r_{\text{H}} = 4''7$, units.

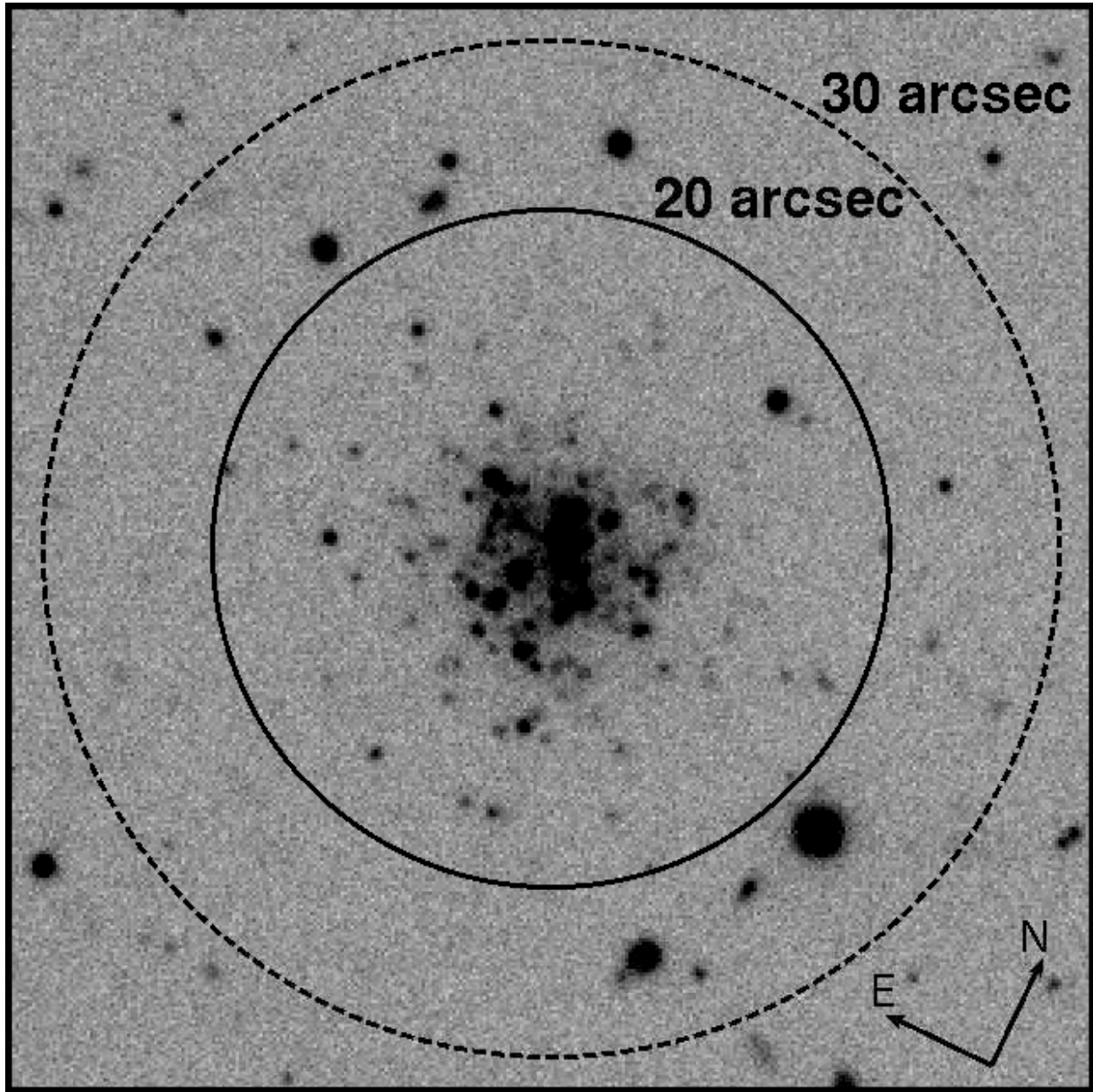


Fig. 1.— Suprime-Cam *R*-band image of the star cluster M33-EC1. The circles indicate radii of $20''$ (solid line) and $30''$ (dashed line), delineating the cluster and the sky background determination areas, respectively.

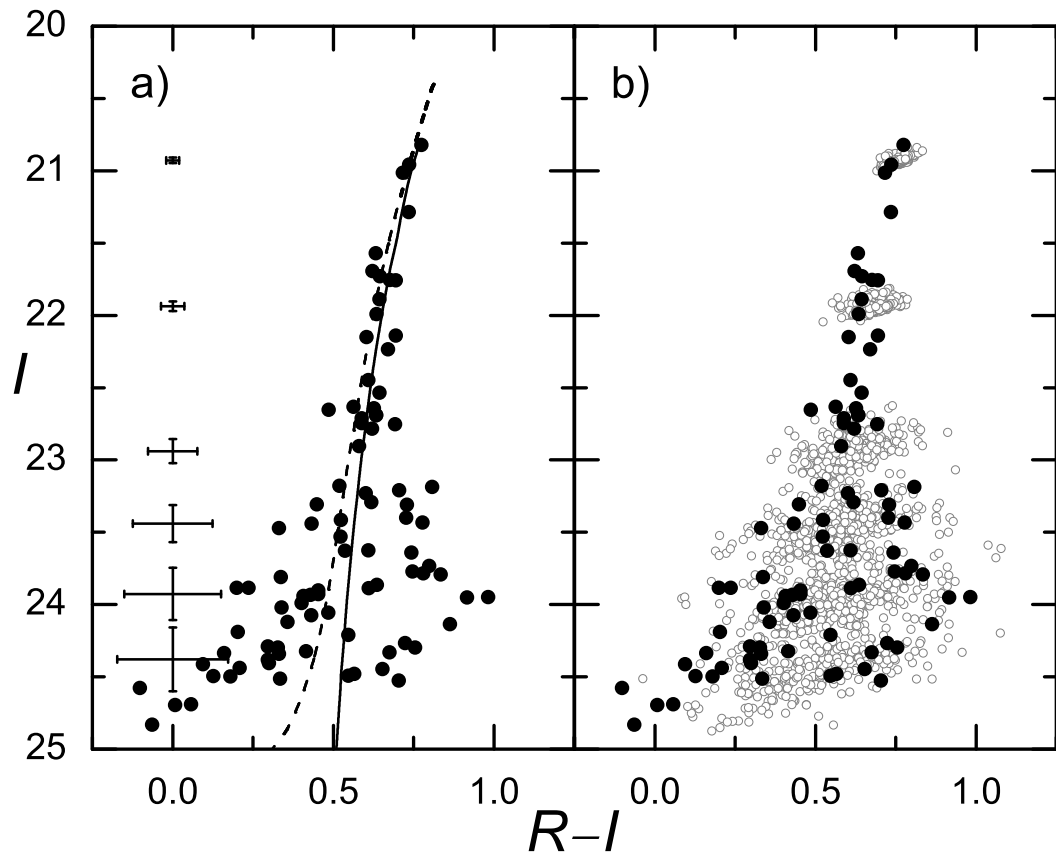


Fig. 2.— The color-magnitude diagram of stellar-like objects residing in the region of $20''$ radius from the M33-EC1 cluster's center: panel a) overlaid with Girardi et al. (2002) isochrone of 14 Gyr and $[M/H] = -1.3$, shifted for distance modulus of 24.75, and reddened according to the foreground MW extinction $A_I = 0.11$, $E(R-I) = 0.045$, (RGB – solid line, AGB – dashed line); panel b) underlaid with the artificial stars (open circles). Error bars shown in the panel a) are derived basing on the artificial star photometry data.

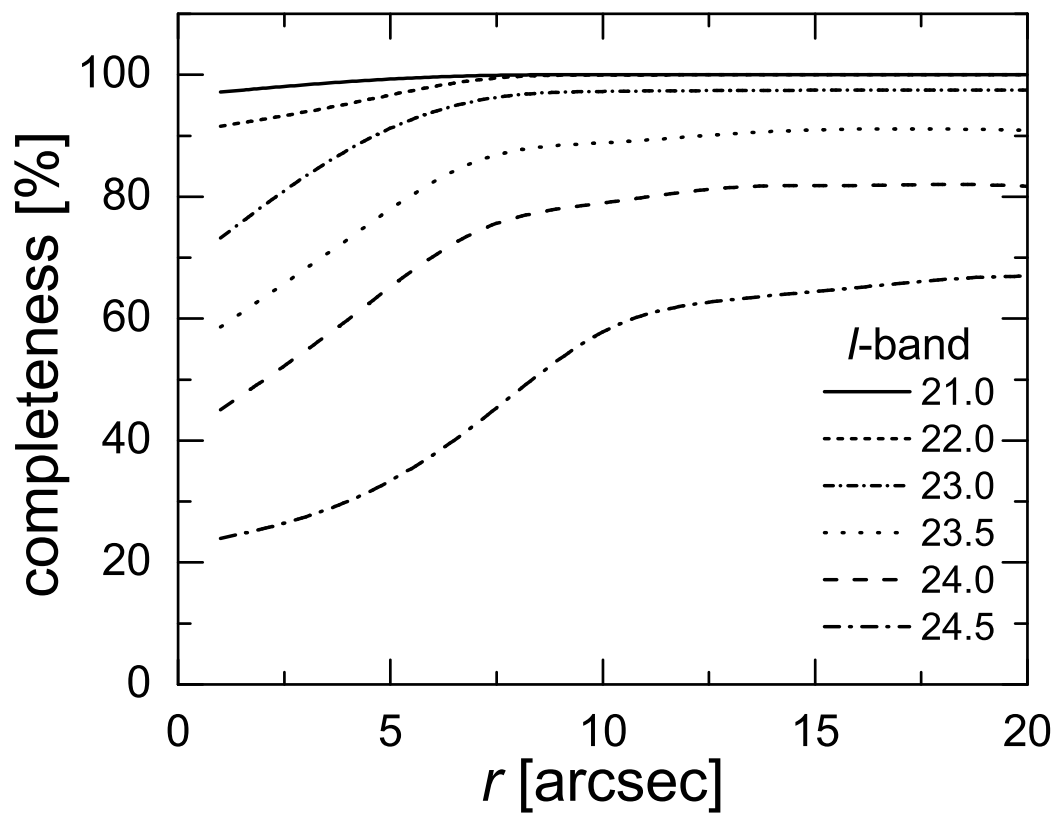


Fig. 3.— Radial dependence of the *I*-band photometry data completeness at the artificial star test (AST) reference points.

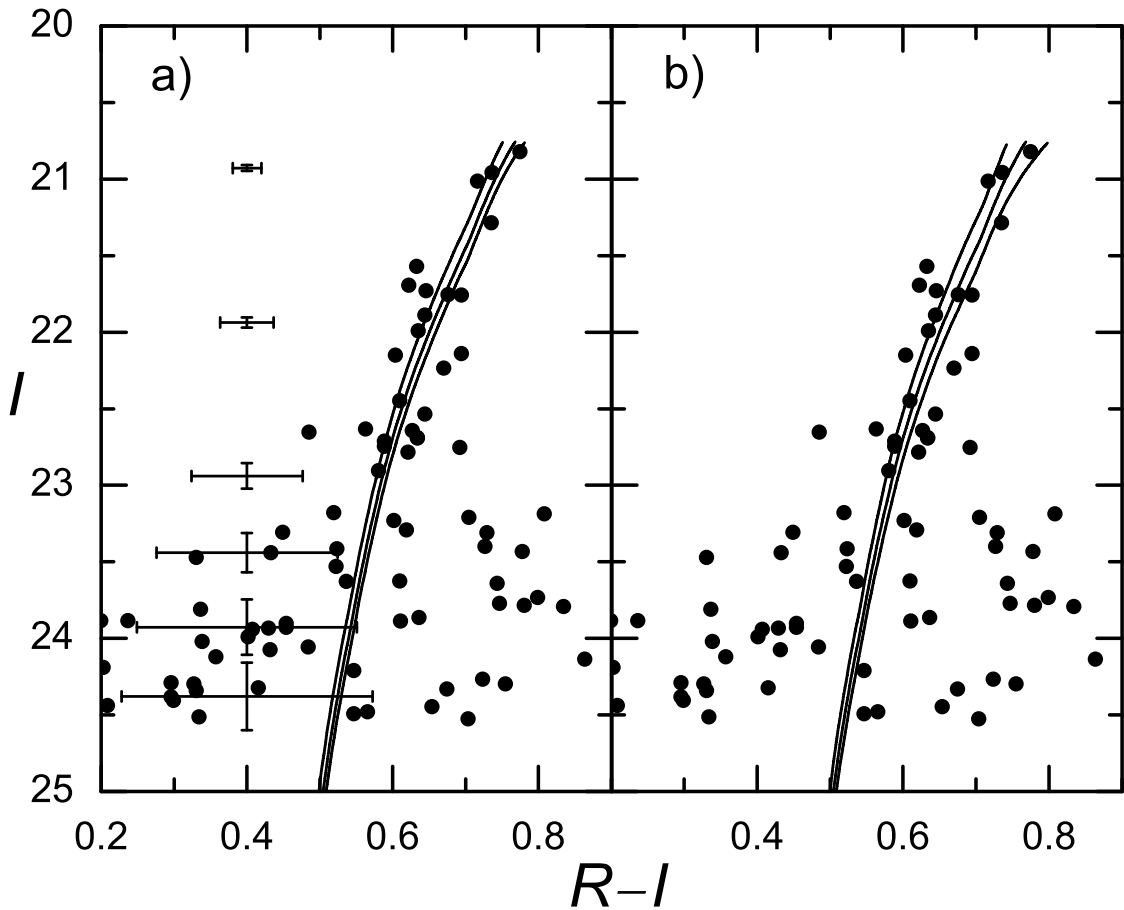


Fig. 4.— The same as in Fig. 2 panel a) but with Vandenberg et al. (2006) isochrones overlaid: panel a) metallicity of $[M/H] = -1.53$ for ages 7, 10, & 13 Gyr; panel b) age of 10 Gyr for $[M/H] = -1.71, -1.53, -1.41$.

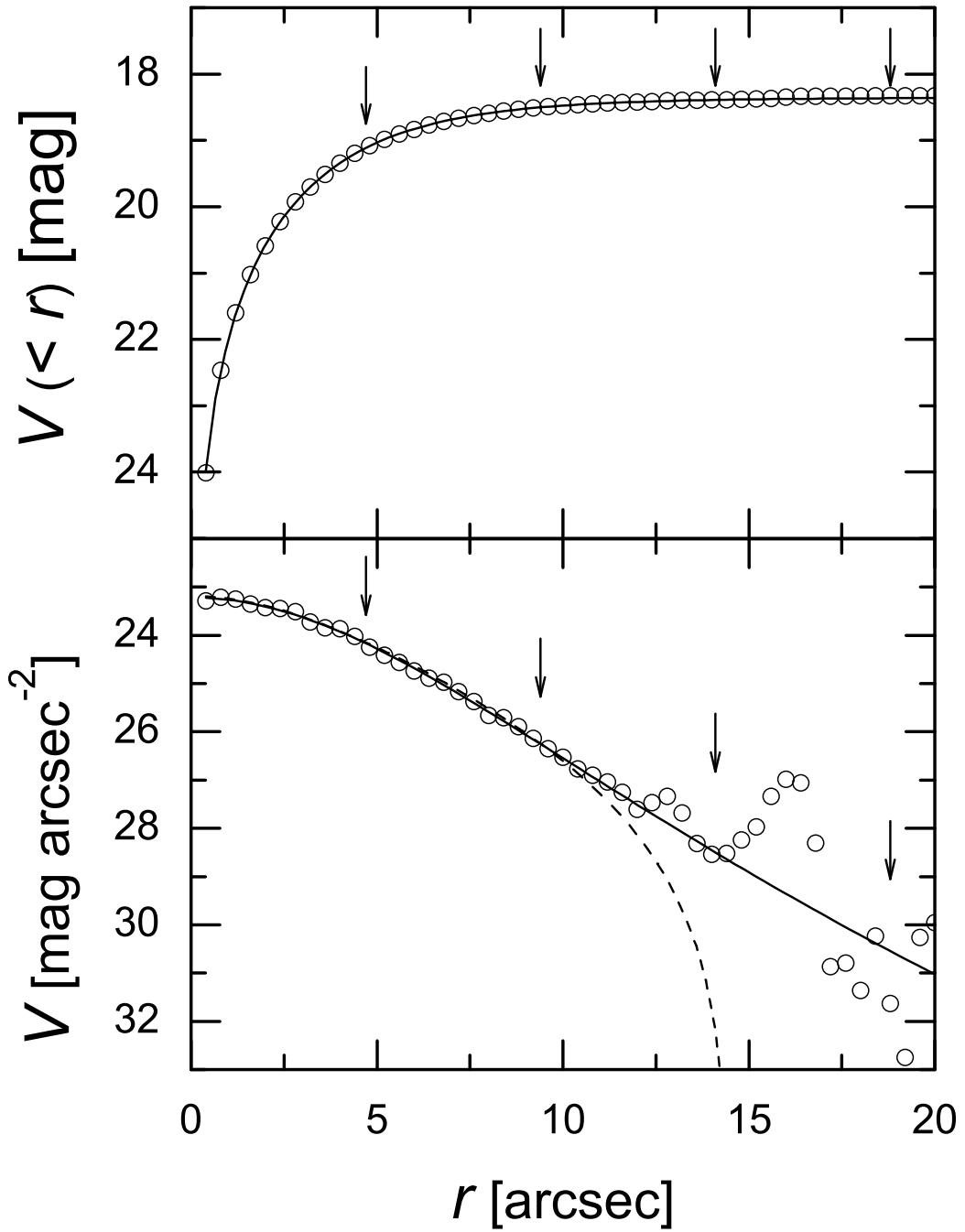


Fig. 5.— The radial profiles of the empirical King (dashed line) and EFF (solid line) model fits to the V -band sky background-subtracted integrated luminosity (top panel) and surface brightness (bottom panel) profiles. Small arrows indicate the radii of $(1, 2, 3, 4) \cdot r_H$; $r_H = 4.7''$.

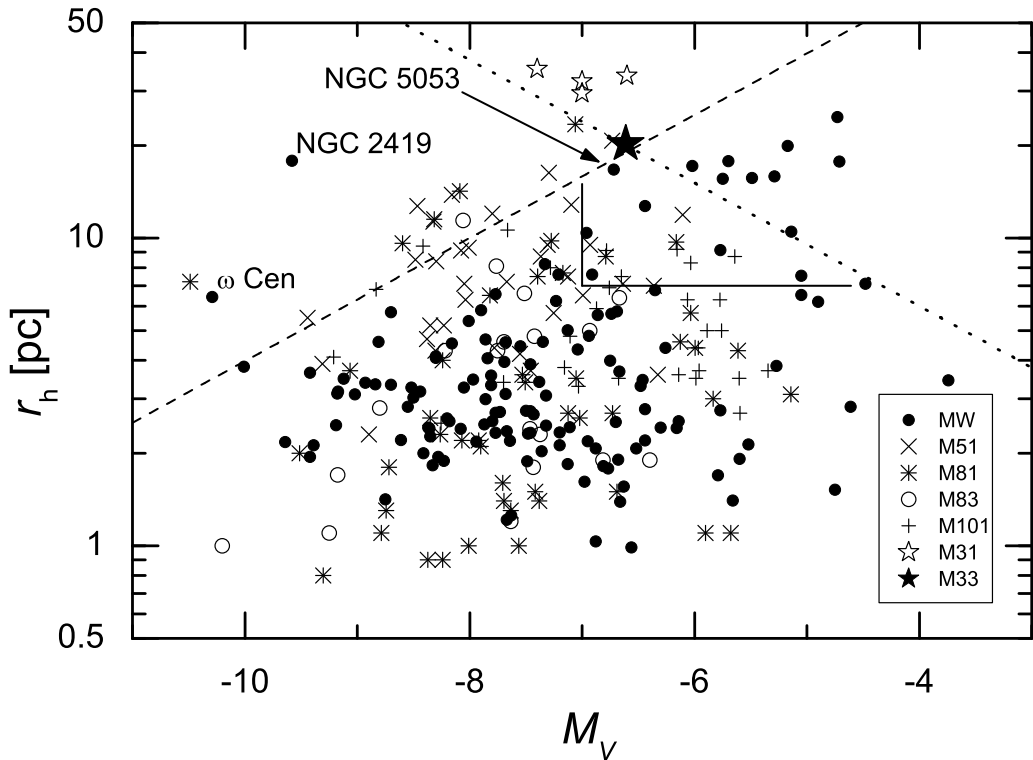


Fig. 6.— Plot of r_h vs. M_V for the eGC M 33-EC1 (filled star). The extended M 31 clusters (Mackey et al. 2006) (open stars), the MW globular clusters (Harris 1996; catalogue revision: Feb. 2003) (filled circles), and clusters in M 51 (crosses), M 81 (asterisks), M 83 (open circles), M 101 (pluses) galaxies (Chandar et al. 2004) are shown. The star clusters of M 33 are not indicated because of their small sizes, $r_c \lesssim 2$ pc (Chandar et al. 1999, 2001). Dashed ($\log(r_h) = 0.2 \cdot M_V + 2.6$; van den Bergh & Mackey (2004)) and dotted (average surface luminosity of $15 \cdot L_{V,\odot} \cdot \text{pc}^{-2}$ within r_h) lines are drawn for reference. The solid L-shape line marks a location of faint fuzzy clusters (Brodie & Larsen 2002). The MW globular clusters ω Cen, NGC 2419, and NGC 5053 are labelled.